Available online at www.sciencedirect.com
SCIENCE DIRECT
Journal of Catalysis 238 (2006) 342–352
JOURNAL OF CATALYSIS
www.elsevier.com/locate/jcat

Selective photo(catalytic)-oxidation of cyclohexane: Effect of wavelength and TiO_2 structure on product yields

Peng Du, Jacob A. Moulijn, Guido Mul *

Reactor and Catalysis Engineering, DelftChemTech, Delft University of Technology, Julianalaan 136, 2628 BL Delft, The Netherlands

Received 26 July 2005; revised 25 November 2005; accepted 9 December 2005

Available online 27 January 2006

Abstract

The liquid-phase photolytic oxidation of cyclohexane was studied and compared with photocatalytic oxidation over TiO_2 with varying wavelengths of light exposure, slurry densities, and sources and pretreatments of catalyst material. Photolytic oxidation at $\lambda < 275$ nm (i.e., in the absence of catalyst) yielded a high selectivity to cyclohexanol (>85%). By adding a TiO_2 catalyst to cyclohexane exposed at $\lambda < 275$ nm, the selectivity shifted to the ketone, with the amount of catalyst added determining the obtained cyclohexanone:cyclohexanol ratio. When a combination of a TiO_2 catalyst and a Pyrex reactor was used (the latter preventing photolytic formation of cyclohexanol), an almost complete selectivity to cyclohexanone was obtained (>95%). The activity toward ketone formation was affected by catalyst structure, with surface hydroxyl group density being the most important parameter. Based on the observed correlation between the hydroxyl group density and activity, as well as the observed negative effect of cyclohexanol addition on cyclohexanone production rate, a preliminary reaction mechanism is proposed involving the light-induced formation of surface cyclohexyl radicals, followed by formation of a peroxide intermediate and decomposition and desorption to cyclohexanone. Accumulation of cyclohexanol on the TiO_2 surface is proposed to deteriorate the photocatalytic activity and to contribute to CO_2 formation.

Keywords: Cyclohexane; Photocatalysis; Oxidation; TiO_2; Hydroxyl groups; Wavelength; Mechanism; Photoreactor

1. Introduction

Heterogeneous photocatalysis has been a subject of a vast amount of studies related to environmental abatement, such as air cleaning and water purification, in which organic pollutants are totally degradated to carbon dioxide and water over mainly TiO_2 photocatalysts [1–3]. Relatively fewer studies were conducted on the application of photocatalysis for product synthesis by selective oxidation. These studies demonstrate that high selectivities can be obtained in TiO_2 photooxidation as compared with conventional oxidation processes [4,5]. A reaction that was of particular interest in previous studies describing liquid-phase photocatalytic selective oxidation was the oxidation of cyclohexane to cyclohexanone and cyclohexanol. Liquid-phase oxidation of cyclohexane is an important commercial reaction in the conversion of cyclohexane via cyclohexanone in caprolactam, a monomer for nylon-6 production. A low cyclohexanol:cyclohexanone ratio is preferred by caprolactam producers, because the consecutive step of cyclohexanol dehydration to cyclohexanone is a costly and energy-consuming process. Table 1 gives an overview of studies that have applied photon energy to selectively oxidize liquid cyclohexane. A first indication of selective photooxidation of cyclohexane by semiconductor oxides was presented in a brief report by Giannotti et al. [6], in which the photocatalytic activities of anatase as well as rutile phases were mentioned. High ketone selectivities were reported of 100% (no CO_2 and cyclohexanol) for anatase and 90% (only 10% CO_2) for rutile. The type of reactor was not discussed, however. In the late 1980s, Mu et al. [7] performed a comprehensive study on this reaction using Degussa P25 TiO_2, which consists of approximately 70% anatase and 30% rutile. Again, high selectivities to cyclohexanone were observed, namely 83% selectivity to the ketone, 5% to the alcohol, and 12% to CO_2. This study was extended to other hydrocarbons and further evaluated by Hermann et al. in 1991 [8].

* Corresponding author.
E-mail address: g.mul@tnw.tudelft.nl (G. Mul).

0021-9517/$ – see front matter
doi:10.1016/j.jcat.2005.12.011

Table 1
Summary of open resources on selective photocatalytic oxidation of cyclohexane over titania

Reference	Catalyst	Reactor/ filter	Illumination source	C_6H_{12} (ml)	Solvent	Time (h)	Conversion (%)	Selectivity (%)		
								$C_6H_{12}OH$	$C_6H_{10}O$	1/6 CO_2
[6]	TiO_2 (anatase) 0.1 g	?	1000 W Hg–Xe	3	–	20	0.09	0	100	0
[6]	TiO_2 (rutile) 0.1 g	?	1000 W Hg–Xe	3	–	20	0.095	0	91.1	8.9
[7,8]	TiO_2 (P25)	$\lambda > 300$ nm	125 W Hg	10		3	0.3	5	83	12
[9]	TiO_2 (anatase) 30 mg	Quartz	250 W Hg	10	–	3	0.05	5.5	92.2	2.3
[12]	Ultrafine TiO_2 30 mg	Quartz	250 W HP Hg	10	CH_3CN 10 ml + HNO_3 1 mol	8	0.096	85.3	14.7	–
[10]	TiO_2 (P25) 4 g/dm^3		400 W MP Hg ($\lambda > 360$ nm)	–	–	1.5	0.078	0	99.1	0.9
[11]	TiO_2 (P25) 20 mg	Pyrex	450 W Xe	20	–	0.75	0.035	19	82	–
[13,14]	Nanosized TiO_2 30 mg	Quartz	250 W Hg	10	CH_3CN 10 ml	3	0.097	84.5	14.9	0.6

Similar product selectivities, with ketone being the major product, were reported in more recent studies of Lu et al. [9], Boarini et al. [10], and Almquist and Biswas [11]. Lu et al. [9] compared the performance of TS-1 and TiO_2, and Boarini et al. [10] and Almquist and Biswas [11] focused mainly on the effect of different solvents on catalyst activity and selectivity in cyclohexane photooxidation over TiO_2. Generally the high ketone selectivity is explained by strong adsorption on titania and higher reactivity of cyclohexanol versus cyclohexane, which undergoes further oxidation toward cyclohexanone or CO_2 as the final product [7–11].

Contradictory results also exist in the open literature. Su et al. [12] and Li et al. [13,14] obtained mainly cyclohexanol by photoactivation of cyclohexane with molecular oxygen, applying nanosized TiO_2 particles. These authors discussed the discrepant performance compared with previous studies on the basis of a quantum size effect and a different surface structure of the used nanosized TiO_2, which supposedly prevents consecutive reaction of cyclohexanol to cyclohexanone [12–14]. From these previous studies, we can conclude that the product distributions reported for photooxidation of neat cyclohexane with TiO_2 catalysts are far from consistent and need further evaluation.

It is remarkable that none of the aforementioned studies systematically compared the photolytic (i.e., without catalyst) and photocatalytic oxidation products in terms of photon efficiency and selectivity. The effect of the applied wavelengths on catalyst performance also was typically not addressed [15,16]. The present study investigates neat cyclohexane photooxidation, varying the reactor setup (quartz, Vycor, or Pyrex immersion wells), affecting the wavelengths available for reaction, as well as the amount and constitution of the applied titania (Degussa P25 and Hombicat pretreated at various calcination temperatures). We show that photolysis and photocatalysis lead to very different product distributions, and that the surface hydroxyl group density on TiO_2 is an important factor in controlling the reaction rate.

2. Experimental

2.1. Applied catalyst materials and catalyst characterization

Degussa P25 titanium dioxide and Hombicat UV100 titania (Sachtleben) were used as photocatalysts. Characteristics of the Hombicat TiO_2 (100% anatase as determined by XRD), include a S_{BET} of 337 m^2/g and primary particle size of ∼5 nm (determined using Scherrer's equation), with a mean agglomerate size in cyclohexane after ultrasonication of ±3 μm (as determined by forward light-scattering). The Hombicat was further pretreated at various temperatures in the range of 400–1273 K in a static oven in air for 12 h, typically at a heating rate of 10 K/min. The various catalyst samples were analysed by various techniques, including UV/vis, XRD, pore texture analysis, and ammonia TPD, to allow evaluation of the structure of the applied TiO_2 and the resulting performance in cyclohexane oxidation.

Cyclohexane UV absorption spectra were measured on a Cary-5 UV–vis spectrometer using a 1-cm quartz transmission cell. The spectra of the solids were recorded at ambient temperature in diffuse reflectance mode, using $BaSO_4$ as a reference. Samples were ground, heated overnight at 180 °C, and scanned from 190 to 800 nm. Powder X-ray diffraction (XRD) patterns were measured on a Philips PW 1840 diffractometer equipped with a graphite monochromator using Cu-K_α radiation ($\lambda = 0.1541$ nm). Nitrogen adsorption and desorption isotherms were recorded on a QuantaChrome Autosorb-6B at 77 K. Samples were previously evacuated at 623 K for 16 h (at a ramp rate of 10 K/min). The BJH model was used to calculate the pore size distribution from the adsorption branch, and the BET method was used to calculate the surface area (S_{BET}) of the samples. Temperature-programmed desorption of ammonia (NH_3-TPD) was carried out on a Micrometrics TPR/TPD 2900 apparatus equipped with a thermal conductivity detector (TCD). Approximately 25 mg of TiO_2 was flushed with helium at 773 K for 1 h (at a heating rate of 10 K/min), except for the sample activated at 398 K, which was pretreated at this temperature in the ammonia TPD setup. After pretreatment, the sample was rapidly cooled to 373 K and loaded with ammonia, applying a flow of 30 ml/min for about 60 min, after which a helium flow of 30 ml/min was applied to remove weakly adsorbed NH_3. A linear temperature program was started (373–873 K at 10 K/min), and the desorbed amount of ammonia was analyzed by the TCD. The TPD spectra were used to determine the nature and amount of hydroxyl groups present on each catalytic material.

A second procedure to determine OH group density on the surface of the applied TiO_2 was based on the $Fe(acac)_3$ method

described by Van Veen et al. [17]. Typically, 0.005 g of catalyst was added to 10 ml of 0.25 mmol/l $Fe(acac)_3$ solution in toluene and stirred in the dark overnight. After this, the solid was centrifuged off, and the supernatant solution was subjected to UV absorption measurements. The amount of adsorbed $Fe(acac)_3$ was determined by comparing the UV absorption at 355 nm with calibrated samples.

2.2. Reactants and solvents

Cyclohexane, cyclohexanol, and cyclohexanone were purchased from Merck. Cyclohexyl hexanoate was purchased from Alfa Aesar, and 1,1′-oxybis(cyclohexane) was synthesized and purified following the procedure of Olah et al. [18]. Anhydrous hexadecane, used as the internal standard for gas chromatography, was purchased from Aldrich. All commercial chemicals were of analytically pure grade and were dried on silica gel before the experiments.

2.3. Photo-activity measurements

To evaluate the effect of wavelength on the selectivity of the reaction, reactions were carried out in a 1000-ml semi-batch slurry-type photochemical reactor with an immersion well (ACE Glass) located in a dark fume hood. The reactor vessel was covered with aluminium foil to prevent the influence of stray light. Illumination was provided by a 450 W medium-pressure mercury-vapor lamp with 39% of total radiated energy in the UV spectrum, also supplied by ACE Glass. During operation, distilled water was circulated through the immersion well for cooling purposes. The temperature inside the reaction vessel was regulated at 333 K through a circulating bath. A Pyrex, Vycor, or quartz cooling jacket was used, with the choice affecting the wavelengths that were available to illuminate the reaction mixture. UV transmission of the applied reactor materials (Pyrex, Vycor, and quartz) was measured using a calibrated Avantes spectrophotometer S-2000 with a UV/vis cosine collector.

In a typical experiment, 600 ml of cyclohexane, along with 1 g of hexadecane as the internal standard, was mechanically stirred together with a desired amount of catalyst, typically 1 g/l. Air was bubbled through the liquid at a rate of 300 ml/min through a gas sparger. Evaporative losses of organics were minimized by applying a reflux condenser. A carbon dioxide trap with saturated barium hydroxide solution was installed to determine the amount of carbon dioxide produced in the form of precipitated barium carbonate.

GC samples were taken from gas and organic phases separately, applying the appropriate syringes. Organic compounds were identified by GC-MS (Chromopack, CP Sil-5) and quantatively analyzed twice using a gas chromatograph with a flame ionization detector (Chromopack, CPwax52CB). Quantification of the oxygenated products in the liquid phase was derived from a multipoint calibration against the internal standard. The following products were thus analyzed quantitatively: cyclohexanol, cyclohexanone, 1,1′-oxybis-cyclohexane, and cyclohexyl hexanoate. CO_2 was analyzed by a gas chromatograph equipped with a TCD, using a Poraplot column. Comparable results were obtained with the $BaCO_3$ precipitation method and the GC analysis. GC quantification is preferred, because it results in more data points and is less labor-intensive.

Cyclohexyl hydroperoxide (CHHP) was detected indirectly according to the procedure of Shul'pin et al. [19]. It was assumed that CHHP was totally converted to the corresponding alcohols and ketones by the addition of an excess of triphenolphosphine. The measurement is useful mainly for qualitative analysis, because of the partial decomposition of CHHP in the gas chromatograph injector and column.

Because of the large amount of liquid reagent in the commercial slurry reactor and the need for cooling to control the reaction temperature, a small slurry system, containing 100 ml of cyclohexane and consisting of a "top illumination reactor" with sophisticated temperature and flow control, was used to evaluate the effect of the catalyst constitution. The solution was illuminated from the top of the reactor through a Pyrex window that cut off the undesired UV radiation. The lamp used in the top illumation reactor was a 35 W Xe–Hg high-intensity discharge lamp (Philips D2/D2S) equipped with an incandescent reflector. The catalyst amount was varied between 0 and 2 g/l. Air, presaturated with cyclohexane at the reaction temperature, was bubbled through the liquid at a rate of 30 ml/min. During reactions, both gas and liquid samples were withdrawn and analyzed by GC.

3. Results

3.1. Characteristics of the applied reactor materials: wavelength variation

Fig. 1 depicts the onset of the UV absorption by neat cyclohexane at 250 nm. Below this wavelength, high light absorption is observed. The figure also shows the transmittance of different glass types and the emission spectrum of the Hg lamp. A large transmittance for quartz at wavelengths in the UV-C region ($\lambda < 280$ nm) was found; thus, a considerable amount of the UV-C irradiation from the Hg lamp can be absorbed directly by cyclohexane in the event that a quartz immersion well is applied. In contrast, transmittance of the Vycor glass and Pyrex starts at values of 220 and 275 nm, respectively, the latter removing the radiation that would activate the cyclohexane directly, thus eliminating photolysis processes. In what follows we show that this has a dramatic influence on the selectivity of the products observed in the catalytic cyclohexane oxidation.

3.2. Cyclohexane photolysis (no catalyst)

The results of photolytic oxidation of cyclohexane in the absence of catalyst, using the quartz immersion well, are illustrated in Figs. 2a, 2b and 3. Cyclohexanol was formed with an order of magnitude higher yield over cyclohexanone and other products, as can be seen by comparing the vertical scales in Figs. 2a and 2b. The slightly S-shaped plot (Fig. 2a) of the cyclohexanol yield indicates a short induction period, most likely related to initiation of the radical reaction and/or heating time of the applied lamp. This is

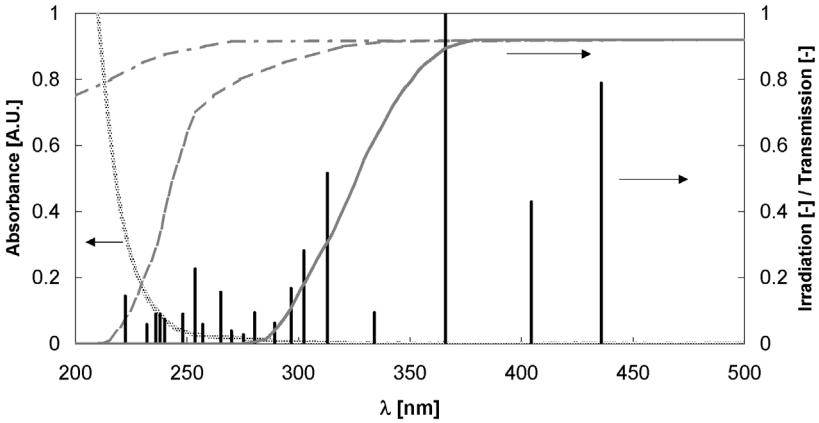

Fig. 1. Comparison of the absorption spectrum of liquid cyclohexane and the UV transmittance of different glass types. From left to right, quartz, Vycor, and Pyrex. Also shown is the line spectrum of the applied Mercury lamp. Intensities are normalized to the maximum emission at 366 nm.

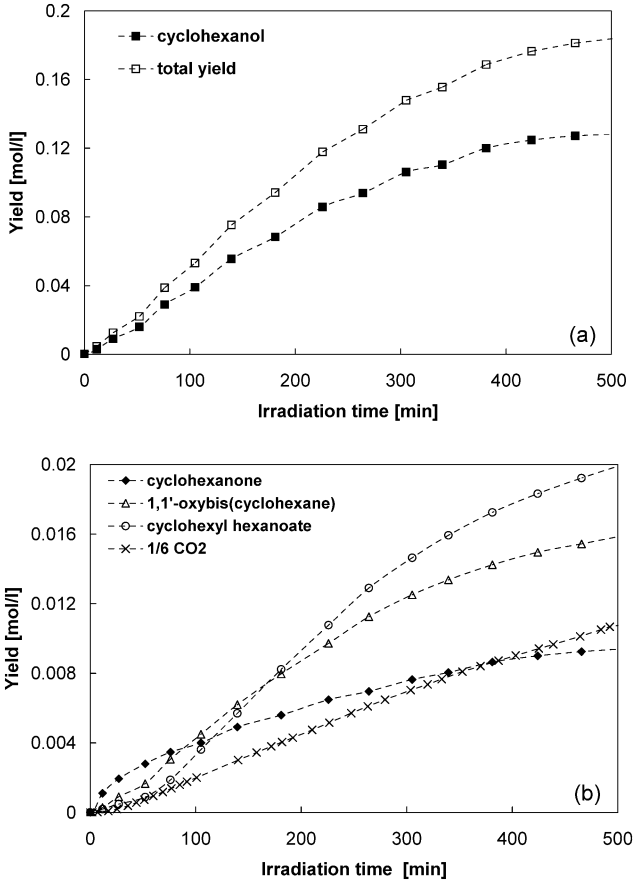

Fig. 2. (a) The yield of cyclohexanol compared to total yield as a function of illumination time. Legend as indicated in the figure. (b) The yield of, respectively, cyclohexanone, 1,1′-oxybis(cyclohexane), cyclohexylhexanoate, and CO_2 (1/6). Legend as indicated in the figure.

followed by a constant rate of cyclohexanol production for up to about 3 h of reaction time, then a significant leveling off of the production rate occurs, related to chain propagation reactions inducing the formation of oligomeric carbon deposits, appearing as a brownish layer on the outer sleeve of the immersion well. Thus, the drop in oxidation rate can be attributed to a reduced photon flux to liquid cyclohexane.

The formation rates of the other products merits further discussion. Fig. 2b shows that other products include 1,1′-oxybis(cyclohexane), cyclohexanone, cyclohexyl hexanoate, and carbon dioxide. The formation of 1,1′-oxybis(cyclohexane) is explained by the etherification reaction of two cyclohexanol molecules, producing water. This ether formation is probably the result of radical processes involving $C_6H_{11}O^{\cdot}$ free radicals.

The high initial rate of cyclohexanone formation demonstrates that cyclohexanone is a primary oxidation product of cyclohexane. Further photooxidation of the ketone proceeds much more rapidly than that of cyclohexane [20], explaining the rapid levelling off of the yield as a function of irradiation time, as shown in Fig. 2b. Cyclohexyl hexanoate, the esterification product of cyclohexanol and hexanoic acid, arises, most likely due to oxidation of cyclohexanone to hexanoic acid. We verified that the cyclohexyl hexanoate is a secondary product of cyclohexanone photolysis by adding cyclohexanone to the reaction mixture. Initially, a decrease in the cyclohexanone concentration was observed, and the amount of cyclohexyl hexanoate was greatly enhanced compared with the results shown in Fig. 2b. The yields of 1,1′-oxybis(cyclohexane), cyclohexanol, and CO_2 were little affected by the addition of cyclohexanone, indicating that these are not related to consecutive cyclohexanone reactions. The origin of carbon dioxide has not been stated clearly in photooxidation studies of cyclohexane, despite the fact that it is the final degradation product. Although it is beyond the scope of the present paper to elucidate and extensively discuss the mechanism of photolysis of cyclohexane, we note that CO_2 is apparently formed from a consecutive reaction of cyclohexanol rather than a consecutive reaction of cyclohexanone.

3.3. *Effect of reactor material on photolysis and photolysis efficiency*

Without going into too much detail on the photolysis reactions with the other reactor materials (Vycor and Pyrex), we note that the highest rate was achieved when a quartz immersion well was applied (Fig. 3). The total yield was reduced by almost half when a Vycor glass well was used, with the product distribution remaining largely unmodified. After most of the

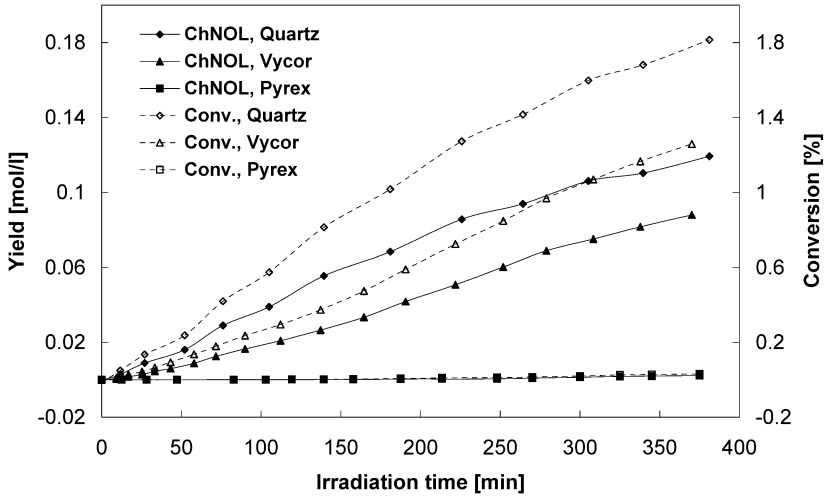

Fig. 3. Cyclohexanol and total yield development with irradiation time, as a function of the applied reactor material. Legend as indicated in the figure.

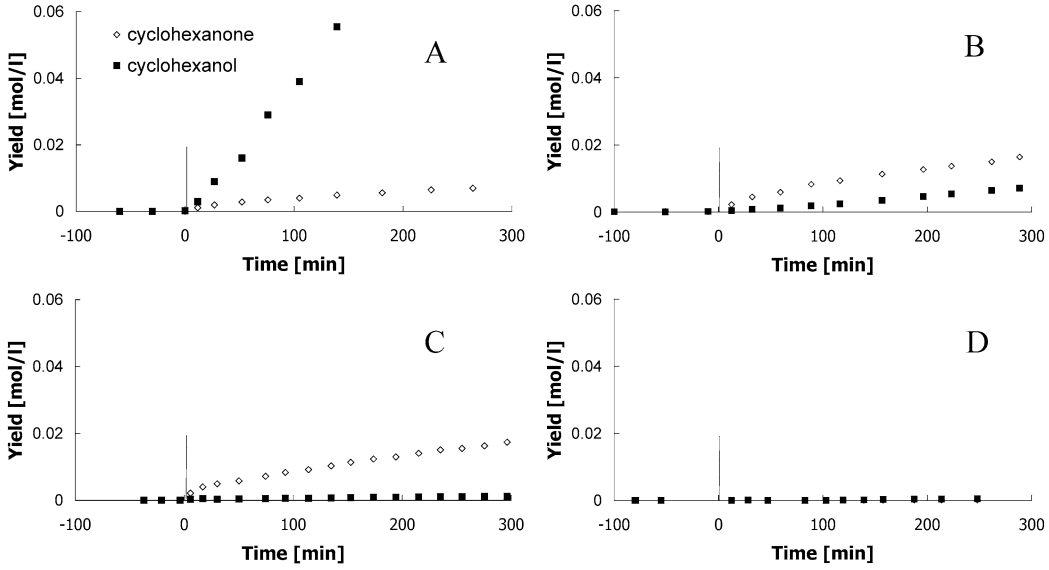

Fig. 4. Effect of the experimental conditions on the cyclohexanone and cyclohexanol amounts produced. (A) Quartz reactor, no catalyst (pure photolysis, cf. Fig. 2), (B) quartz reactor, with catalyst (1 g/l of P25), (C) Pyrex reactor with catalyst (1 g/l of P25), and (D) Pyrex reactor, no catalyst.

UV-B and UV-C radiation was eliminated with the Pyrex immersion well, direct photolysis became negligible. In the latter case, cyclohexanol and cyclohexanone were detected only after 150 min of reaction, and the concentration of CO_2 in the exhaust gas remained below the TCD's detection limit during the entire experiment. Clearly, the energy of individual photons after light filtration was too low to activate cyclohexane molecules to a photoreactive excited state.

The quantum yield for cyclohexanol in photolysis in the quartz reactor, based on the ratio of the reaction rate r (in mol produced per second) and photonic flux expressed by the number of efficient moles of photons, was 14%. This efficiency was significantly affected by introduction of the catalyst, as we discuss next.

3.4. Photocatalytic oxidation of cyclohexane

The effect of the applied reactor material on the product formation of cyclohexane oxidation without (photolysis) and with catalyst (Degussa P25, photocatalysis) is further illustrated in Fig. 4. For simplicity, this figure shows only the cyclohexanol and cyclohexanone in the case of photolysis, neglecting the minor products of consecutive radical chemistry, which generally were not observed in photocatalysis. As stated previously, in the photolysis reaction conducted with the quartz immersion well, cyclohexanol was the major product, with little cyclohexanone formed. When using the Pyrex well (Fig. 4D), photolysis was negligible. When P25 was introduced into the reactor equipped with a quartz well, the product distribution changed dramatically (compare Figs. 4A and 4B). In the presence of the catalyst particles, cyclohexanone became the major product, whereas cyclohexanol production was largely suppressed. When using the Pyrex well (Fig. 4C), cyclohexanol production was practically nil, and cyclohexanone was obtained with high selectivity.

It should be noted that there is no apparent linear initial part in the production curve of cyclohexanone (cf. Fig. 8), which, combined with the fact that the kinetics of the reaction are not

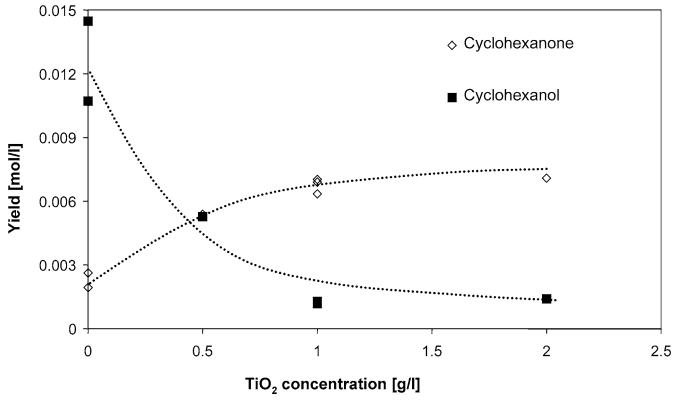

Fig. 5. Effect of the TiO_2 slurry density on the amounts of cyclohexanol and cyclohexanone formed after 60 min of irradiation time in the quartz immersion well reactor.

known, makes the determination of the specific activity (per g of catalyst) or intrinsic activity (per m^2 of catalyst) tedious and possible only with insufficient accuracy. By a rough comparison of the production curves of cyclohexanol and cyclohexanone in Figs. 4a and 4b, the catalytic rate is at least one order of magnitude lower than the photolysis rate, and quantum efficiency is estimated to be in the order of 1–2% in these specific reaction conditions.

Fig. 5 shows the effect of the amount of catalyst in the quartz reactor on the product distribution (cyclohexanone/cyclohexanol). Increasing the amount of catalyst results in increased cyclohexanone production and decreased cyclohexanol production, up to a catalyst density of about 1 g/l, after which the addition of more catalyst has little effect on the quantities produced.

The evolution of CO_2 was evaluated using the maximum amount of 1 g TiO_2/l. Fig. 6a shows the development of the product constitution as a function of reaction time. A significant decrease in reactivity can be observed after about 45 min of illumination. Although not directly apparent from the product distribution shown in Fig. 6a, the evolution of CO_2 is somewhat retarded in the first hour of reaction, leading to an apparent decreasing selectivity of total selective oxidation products as a function of time. This is further illustrated in Fig. 6b, which shows a decrease in selective oxidation products (ketone and alcohol) from >95% to about 85%.

Fig. 7 illustrates that adding cyclohexanol to the reaction mixture decreased cyclohexanone production. Increasing the amount of cyclohexanol from 0.05 to 0.11 g had no further deteriorating effect on the cyclohexanone formation, however.

3.5. *Effect of catalyst constitution on performance*

Besides the amount of catalyst added to the reactor system, the composition of the catalyst also affects the obtained reaction rates. This is illustrated in Fig. 8, which shows the effect of Hombicat pretreatment temperature on performance. In principle, Hombicat TiO_2 is more active than P25, whereas pretreatment of Hombicat at 773 K results in similar activity. Further increases in pretreatment temperature resulted in further deterioration of activity, with activity reduced by a factor

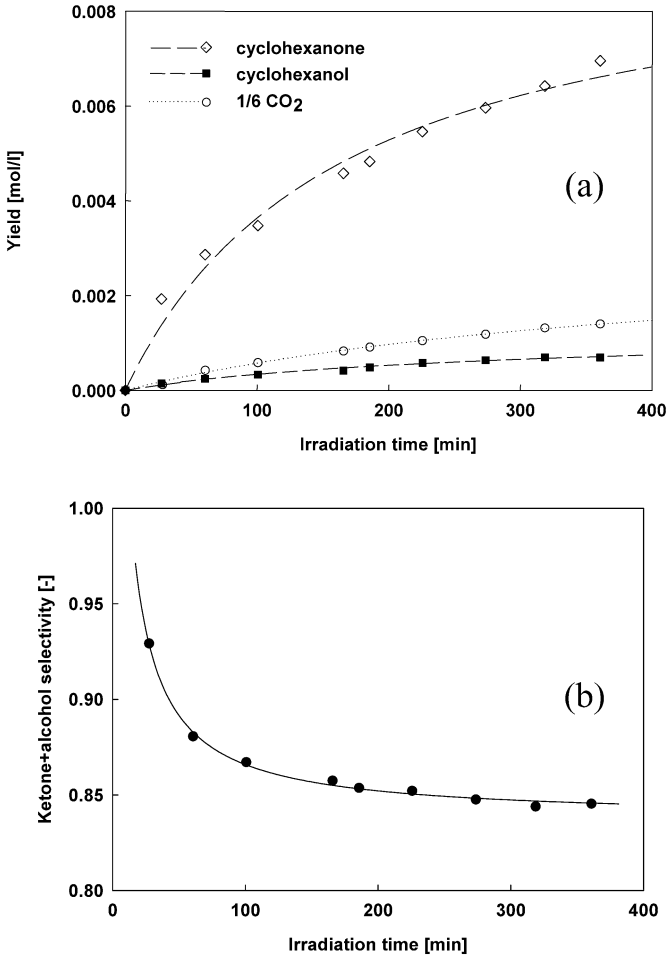

Fig. 6. Product development as a function of irradiation time (1 g/l slurry density of Hombicat catalyst, top illumination reactor). (a) Cyclohexanol, cyclohexanone and CO_2 production (legend as indicated in the figure); (b) selectivity of ketone and alcohol as a function of time.

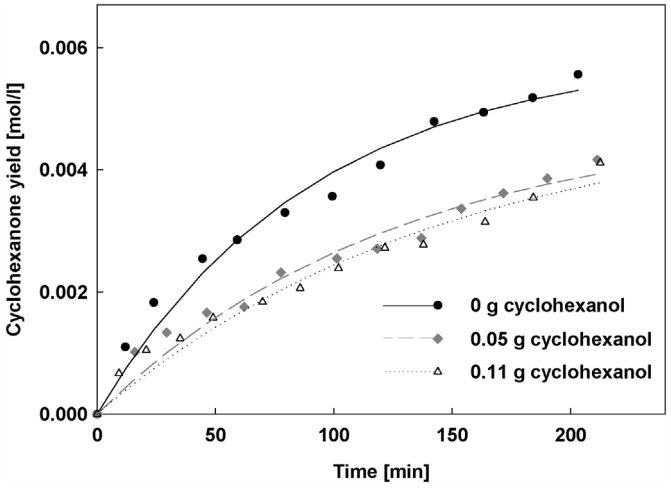

Fig. 7. Effect of preaddition of cyclohexanol (0.5 and 1.1 g) on the cyclohexanone production curve. Reaction conditions: top illumination reactor, 100 ml cyclohexane, 1 g/l slurry density of Hombicat catalyst.

of 2 at 1073 K and almost completely eliminated at 1373 K. Remarkably, the selectivity of the reaction was hardly affected. High-temperature treatment induced various modifications in

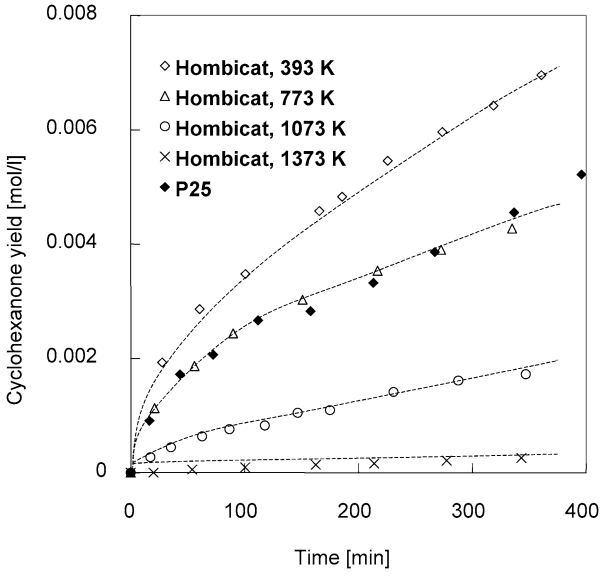

Fig. 8. Comparison of the performance of various TiO_2 samples in the production of cyclohexanone (Hombicat pretreated at respectively 393, 773, 1073 and 1373 K, and P25 treated at 393 K). Legend as indicated in the figure.

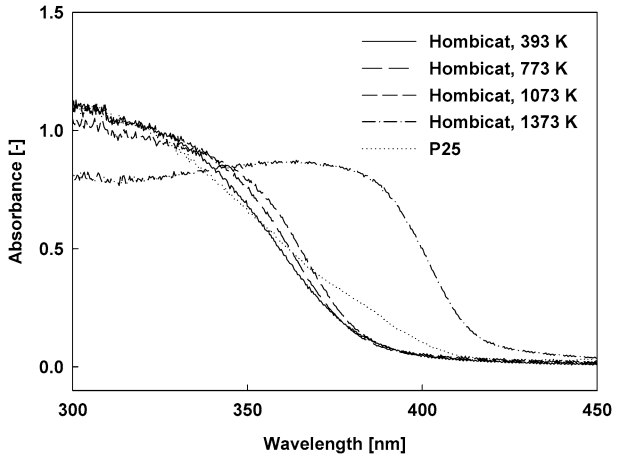

Fig. 9. Effect of the pretreatment temperature of Hombicat on the corresponding UV/vis absorption spectra. Starting from a pretreatment temperature of about 1373 K, a gradual increase of the absorption maximum at 385 nm is induced.

Hombicat, the most important of which were the reduction of the surface area and hydroxyl group density and a phase transition from anatase to rutile above ∼1000 K. We discuss this in more detail in Section 3.6.

3.6. Catalyst morphology as a function of pretreatment temperature

From the XRD diffraction patterns (not shown), it follows that the composition of Hombicat changed from a purely crystalline anatase phase to a rutile phase starting at about 1000 K. At this temperature, a mixed composition of anatase and rutile phases was obtained, whereas above 1273 K, the catalyst consisted predominantly of rutile. Fig. 9 shows the UV absorption spectra of the temperature-pretreated Hombicat samples. Temperature treatments up to about 1000 K had little affect on the absorption spectra. At pretreatment temperatures above 1000 K, the absorption maximum at about 385 nm gradually increased as a function of increasing pretreatment temperature. This enhanced absorbance is related to formation of the rutile phase in the catalysts, as was observed in the XRD patterns of the corresponding materials.

Fig. 10a gives examples of nitrogen adsorption–desorption isotherms of treated Hombicat UV100 samples. All show type II isotherms, indicating some mesoporosity and macroporosity. It is very unlikely that cyclohexane will suffer from restrictions diffusing into these open structures. The absence of a plateau at high relative pressures (p/p_0) indicates the filling of interparticle voids and the presence of surface roughness. Fig. 10b illustrates the decreased surface area of Hombicat as a function of pretreatment temperature, with BET surface area decreasing from 330 m^2/g to only a few m^2/g.

TPD of ammonia (NH_3-TPD) is a very common method for characterizing acidic OH groups in microporous and mesoporous materials [21]. Fig. 11 shows NH_3-TPD spectra of various thermally pretreated titania catalysts. Two desorption maxima can be distinguished at approximately 475 and 600 K. The low-temperature maximum is usually assigned to the removal of ammonia interacting with surface adsorbed water molecules, whereas the high-temperature maximum is correlated with NH_3 associated with the sites created by dehydroxylation of surface OH groups [22]. According to Almquist and Biswas [11], both surface water and hydroxyl groups evenly contribute to photocatalytic oxidation reactions in organic solvent, because in both cases hydroxyl radicals are formed by photogenerated holes. This hypothesis is plausible, because at a surface coverage of 5 H_2O/nm^2 (as is the case for most titania under normal conditions), the fully nondissociated state of water and the fully dissociated configurations can compete in energy within <7 kJ/mol [23]. Therefore, in the discussion that follows, we use "surface OH groups" to designate an OH mode from either Ti–OH or surface-adsorbed H_2O.

Table 2 compares the surface properties of various catalysts. The total surface-OH group quantity of P25 is in good agreement with the quantities reported by Van Veen et al. [17], Chhor et al. [24], and Boehm et al. [25] (the latter of which applied various probe molecules to characterize surface hydroxyl groups on P25 catalysts). As discussed earlier, the performance of the Hombicat pretreated at 773 K is very similar to that observed for P25, pretreated at 393 K. Comparing the data in Table 2 indicates that the number of hydroxyl groups is in much better agreement in the Hombicat 773 K catalyst and the P25 catalyst compared with the BET surface area, and thus is a more important parameter than surface area per se.

4. Discussion

As stated in the Introduction, various groups have evaluated the performance of TiO_2 in the selective oxidation of cyclohexane to cyclohexanol and cyclohexanone (Table 1). The performance of the photocatalysts in the oxidation of cyclohexane is usually discussed only on the basis of the applied catalyst material, with details of the reactors applied and thus

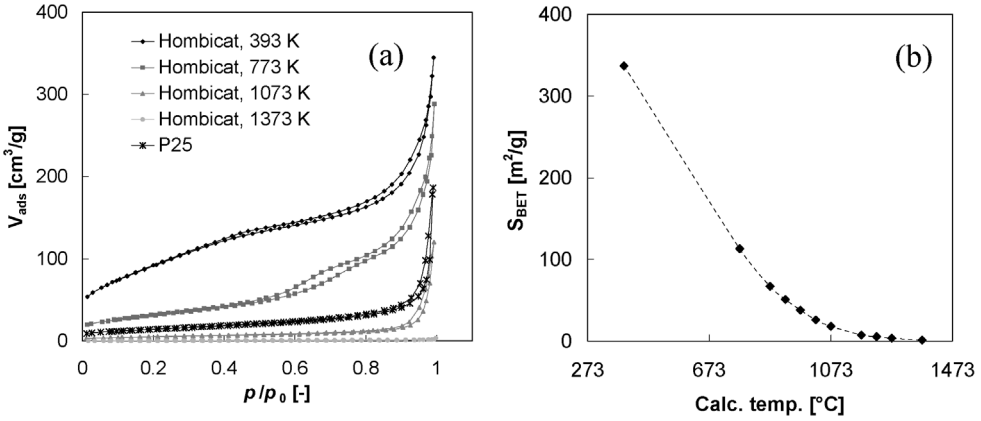

Fig. 10. Nitrogen adsorption–desorption isotherms (a) and the corresponding surface areas as calculated from the BET method (b) of Hombicat pretreated at 393, 773, 1073 and 1373 K, and P25 pretreated at 393 K, respectively.

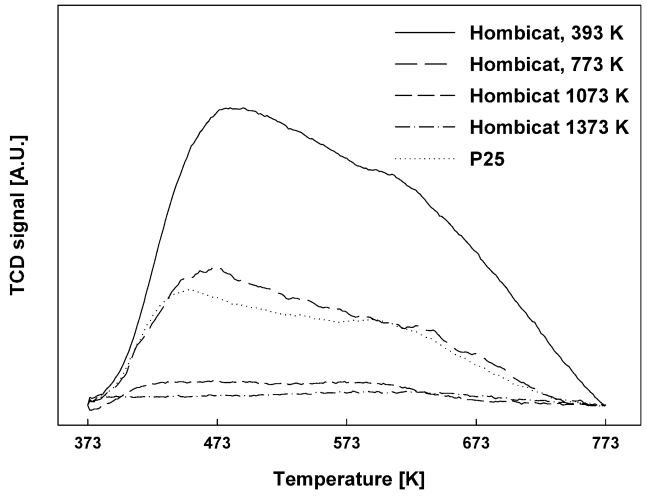

Fig. 11. Ammonia TPD spectra of the applied Hombicat catalysts. Legend as indicated in the figure.

Table 2
Comparison of surface area and OH group density of applied catalysts

	Hombicat				P25
	393 K	773 K	1073 K	1373 K	
Surface area (m^2/g)[a]	337	113	18	1.8	51
Total surface-OH (mmol/g)[b]	1.21	0.40	0.090	0.012	0.38
Acidic-OH (mmol/g)[c]	0.92	0.33	0.070	0.009	0.30
Acidic-OH/basic-OH[b]	3.3	4.7	3.6	3.4	3.6
Surface-OH density (1/nm^2)	2.2	2.1	3.0	3.9	4.5

[a] Determined by nitrogen adsorption and desorption isotherm.
[b] Determined by Fe(acac)$_3$ adsorption method as described by Van Veen et al. [17].
[c] Determined by ammonia TPD.

the wavelengths to which the reaction mixture is exposed not mentioned. The most important finding of the present study is that varying the applied reactor material and the applied slurry density greatly affects the selectivity of the photocatalytic oxidation of cyclohexane, which can vary from >85% selectivity to cyclohexanol for photolytic oxidation to >95% selectivity to cyclohexanone for photocatalytic oxidation. This is clearly illustrated by the results presented in Figs. 1–5.

When a quartz reactor and no catalyst are used, photolysis of cyclohexane is possible at wavelengths $\lambda < 275$ nm. Along with the main product, cyclohexanol, various other products are obtained in the photolysis of cyclohexane, which, as discussed previously, are most likely the result of radical chemistry. The radical pathways, which have been discussed previously [10,11], can describe the observations in the present paper. This radical chemistry is also responsible for the formation of oligomeric carbon deposits on the walls of the immersed lamp, leading to reduced reaction efficiency.

When catalytic material (TiO_2) is added to the reactor, depending on the amount, catalytic surface reactions become dominant over photolysis radical reactions, and the various products of coupling reactions are below the detection limit of the applied analytical procedures. The overall product amount is decreasing as a result of inefficient light absorption by the catalyst particles, in which to a large extent the generated holes and electrons (representative of the activated state) are recombining to produce heat, rather than induce chemical conversion. As discussed earlier, this results in a loss of photoefficiency of at least one order of magnitude. To completely exclude the radical chemistry induced by photolysis, and to obtain an as high a cyclohexanone selectivity as possible, Pyrex should be used as the reactor material to prevent illumination of the reaction mixture to wavelengths <275 nm, as indicated by the product distributions in Fig. 4. In view of this, along with the observed solvent effects reported previously [10,11], it is likely that the nanoparticle effect to explain selectivity changes claimed by Su et al. [12] and Li et al. [13,14] is nonexistent, and that the reversed selectivity reported previously [12–14] is the result of the applied reactor material (quartz), and possibly the addition of acetonitril to cyclohexane. The high selectivity in the photocatalysis of cyclohexane oxidation to cyclohexanone has been extensively discussed in the literature. The consecutive reaction of cyclohexanol to cyclohexanone has been proposed to explain the high selectivity to cyclohexanone [7–11], whereas the high selectivity to cyclohexanone may also be related to a preferred direct catalytic route of cyclohexane oxidation, as proposed by Boarini et al. [10]. From the results of the present study, we

can postulate that the direct route (parallel formation of cyclohexanol and cyclohexanone) is more likely, as we discuss next.

As stated previously, the reaction rate significantly decreased as a function of reaction time using TiO_2 as a photocatalyst (Fig. 6). This cannot be the result of first-order cyclohexane behavior, because the conversion of cyclohexane is very low. Rather, this reaction profile suggests that products are accumulating on the catalyst surface, reducing the effectiveness of the photocatalyst. Results of the experiments in which cyclohexanol was preadded to the reaction mixture show that cyclohexanol inhibits cyclohexanone formation, in agreement with previous observations and with the results of Almquist and Biswas [11]. Furthermore, in preliminary infrared studies, it was observed that cyclohexanol is strongly adsorbed on the catalyst surface, as was also proposed by Almquist and Biswas [11]. However, adsorbed cyclohexanol is photocatalytically converted mainly to carboxylates and not to cyclohexanone, in agreement with IR studies on TiO_2 catalysts that found adsorbed alkoxygroups to be prone to formate and acetate formation on the surface, being precursors of CO_2 [26]. This finding is in good agreement with the decreasing selectivity as a function of reaction time observed in the present study (Fig. 6b). The coproduct cyclohexanol indeed accumulated on the surface, but yielded mainly carboxylates and induced deactivation, rather than contributing to cyclohexanone formation to any great extent.

4.1. Effect of catalyst pretreatment on cyclohexanone production

It is evident from the various characterization techniques that a high-temperature treatment has a significant effect on both catalyst composition (rutile or anatase) and catalyst texture. The transition of anatase to rutile induces enhanced light absorption at relatively high wavelengths by the catalyst (Fig. 9); however, this does not lead to enhanced cyclohexanone formation. Apparently, light absorption in rutile phases is less effective in inducing catalytic reaction than anatase, because of the morphological changes accompanying the transformation of anatase to rutile. A comparison of the performance and constitution of the Hombicat catalysts pretreated at various temperatures with the performance of Degussa P25 is highly illustrative (Fig. 8, Table 2). Comparing the data in Table 2 indicates that the number of hydroxyl groups is in much better agreement between the Hombicat-773 K catalyst and the P25 catalyst, which show comparable activity profiles, than the BET surface area. Thus, it seems that the number of hydroxyl groups is a more important parameter than the surface area per se. Because the kinetic curves are similar, the specific activity can be assumed to be similar, and thus the intrinsic activity (per m^2 of catalyst) of P25 is about twice that of Hombicat-773 K. In other words, compared with Hombicat, P25 effectively accommodates twice the amount of active hydroxyl groups at a comparable surface area (Table 2). At the same time, it can be concluded that the intrinsic activity of each hydroxyl group is independent on the catalyst used (Hombicat-773 K or P25). Based on the determined total amount of surface Ti-hydroxyl groups in the reactor loaded with P25 (0.04 mmol) and a first rough approximation of the corresponding initial photooxidation rate of 0.4 mmol/h (which, as stated earlier, is hard to determine due to the absence of a linear part in the production curve (see Fig. 8)), a turnover of 10 h^{-1} can be calculated for each OH group on the surface. This is a very low number compared with that for, say, homogeneous catalysts with several orders of magnitude higher turnovers.

It should be noted that from Fig. 8, it follows that the activity of the Hombicat catalyst deteriorates continuously as a function of increasing pretreatment temperature. Hisanaga et al. [26] investigated the effect of calcination temperature on photocatalytic performance in relation to water-phase oxidation processes. In water-phase reactions, calcination in the temperature range of 300–773 K typically had little effect or improved photooxidation activity, depending on the solubility of the substrates in water. To explain this improvement, the efficiency of electron and hole charge separation was proposed to be higher in larger crystals (calcination temperature up to 773 K). The effect of calcination temperature on the hydroxyl group density on the TiO_2 surface was not discussed by Hisanaga et al. [26] and appears to be less relevant in water-phase reactions than in neat cyclohexane. Reconstruction of hydroxyl groups by immersion in water is likely, but is more difficult to envisage in pure cyclohexane. If it exists for Hombicat, then apparently the enhanced efficiency of electron hole separation in larger crystals cannot compensate for the reduced hydroxyl group density, explaining the continuously deteriorating efficiency as a function of increasing calcination temperature.

Combining all of the information presented herein, we can propose a mechanism for cyclohexanone formation, as shown in Fig. 12. After adsorption of cyclohexane and the initial activation by light, a reaction occurs between an activated hydroxyl group and cyclohexane, yielding water and an adsorbed cyclohexyl radical. Subsequently, oxygen is activated by the thus-generated Ti(III) center, yielding O_2^-. Recombination of the cyclohexyl radical and the surface O_2^- anion results in the formation of a peroxide intermediate that subsequently decomposes to cyclohexanone and restores the hydroxyl group on the catalyst surface. The formation of peroxides as important intermediates in zeolite-induced selective (photo)oxidation has been extensively described and discussed by Frei and coworkers [27,28], including the reaction of cyclohexane to cyclohexanone [27]. Moreover, cyclohexylhydroperoxide is a common intermediate in the currently applied processes for cyclohexanone production and is known to (catalytically) decompose to either alcohol or ketone [29]. Alternatively, the surface cyclohexylradical might form surface cyclohexanol via photon-induced hydroxyl group activation, but this is speculative. Whatever the pathway to surface cyclohexanol formation, consecutive oxidation, possibly through superoxide anions, leads to carboxylates on the surface, which contribute to deactivation of TiO_2 and also to CO_2 formation. Carboxylates have been previously shown to deactivate Au/TiO_2 catalysts in the low-temperature selective propene epoxidation reaction, using hydrogen and oxygen [30]. It should also be noted that this mechanism is oversimplified; it was previously observed that, depending on the applied solvent, cyclohexanol can be con-

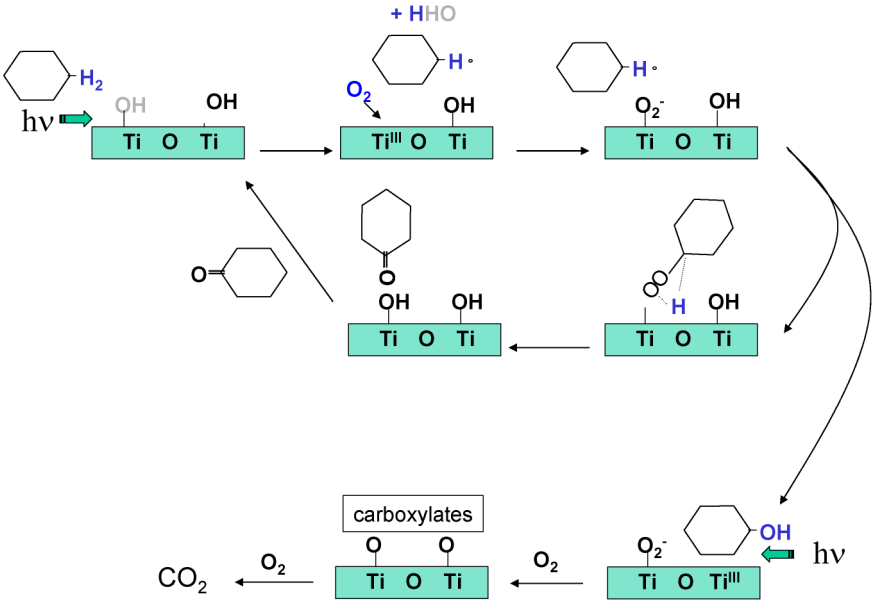

Fig. 12. Reaction scheme proposed for the photo-catalytic production of cyclohexanone over TiO_2 catalysts.

verted photocatalytically to cyclohexanone over TiO_2. Further research, using ATR-FTIR and DRIFT spectroscopy, is ongoing to corroborate the mechanism proposed in Fig. 12, also taking into account the more extensive reaction pathways proposed by other investigators [7–14]. In addition, studies with deuterated cyclohexane and cyclohexyl hydroperoxide are planned to evaluate the kinetic isotope effect and products of peroxide decomposition, respectively, and thus reveal the kinetically relevant step in the photooxidation of cyclohexane to cyclohexanone over TiO_2 catalysts and the extended network of surface photooxidation reactions. Further analysis of the reaction mechanism and kinetically relevant steps may lead to design rules for significantly improved photocatalysts and reactors, which are needed to bring the photocatalytic oxidation of cyclohexane within the range of rates of interest to the chemical industry.

5. Conclusion

The following conclusions can be derived from the work described in this paper:

- Cyclohexanol is the major product of uncatalyzed photooxidation of cyclohexane at $\lambda < 275$ nm. Adding a catalyst suppresses cyclohexanol formation and enhances cyclohexanone formation under these conditions.
- If photolysis is prevented by the use of the proper light filters (e.g., Pyrex, $\lambda > 275$ nm), then photocatalysis over TiO_2 yields predominantly cyclohexanone (selectivity >95%).
- In immersion well-type reactors, as well as in top illumination reactors, an optimized TiO_2 slurry density of about 1 g/l was found. A higher amount shields part of the available reactor volume from the light.
- The textural and chemical composition of the applied TiO_2 was found to have a significant effect on the activity of the catalyst, but no effect on the selectivity. The main variable affecting activity is the hydroxyl group density on the surface of the applied TiO_2, suggesting that hydroxylgroups are directly involved in the kinetically relevant step of the photooxidation of cyclohexane to cyclohexanol.

References

[1] M. Schiavello, Heterogeneous Photocatalysis, Wiley, Chichester, 1997.
[2] O. Carp, C.L. Huisman, A. Reller, Prog. Solid State Chem. 32 (2004) 33–177.
[3] M.R. Hoffmann, S.T. Martin, W. Choi, D.W. Bahnemann, Chem. Rev. 95 (1995) 69–96.
[4] A.K. Suresh, M.M. Sharma, T. Sridhar, Ind. Eng. Chem. Res. 39 (2000) 3958–3997.
[5] A. Maldotti, A. Mollinari, R. Amadelli, Chem. Rev. 102 (2002) 3811–3832.
[6] C. Giannotti, S. Le Greneur, O. Watts, Tetrahedron Lett. 24 (1983) 5071–5072.
[7] W. Mu, J.M. Herrmann, P. Pichat, Catal. Lett. 3 (1989) 73–84.
[8] J.M. Herrmann, W. Mu, P. Pichat, Stud. Surf. Sci. Catal. 59 (1991) 405–414.
[9] G. Lu, H. Gao, J. Suo, S. Li, J. Chem. Soc., Chem. Commun. (1994) 2423–2424.
[10] P. Boarini, V. Carassiti, A. Maldotti, R. Amadelli, Langmuir 14 (1998) 2080–2085.
[11] C.B. Almquist, P. Biswas, Appl. Catal. A 214 (2001) 259–271.
[12] B. Su, Y. He, X. Li, E. Lin, Indian J. Chem. A 36 (1997) 785–788.
[13] X. Li, G. Chen, P.L. Yue, C. Kutal, J. Chem. Technol. Biotechol. 78 (2003) 1246–1251.
[14] X. Li, X. Quan, C. Kutal, Scripta Mater. 50 (2004) 499–505.
[15] M.A. Brusa, M.A. Grela, J. Phys. Chem. B 109 (2005) 1914–1918.
[16] R.W. Matthews, S.R. McEvoy, J. Photochem. Photobiol. A: Chem. 66 (1992) 355–366.
[17] R.J.A. Van Veen, F.T.G. Veltmaat, G. Jonkers, J. Chem. Soc., Chem. Commun. 23 (1985) 1656–1658.
[18] G.A. Olah, T. Shamma, G.K. Surya Prakash, Catal. Lett. 46 (1997) 1–4.
[19] G.B. Shul'pin, D. Attanasio, L. Suber, J. Catal. 142 (2003) 147–152.
[20] I.V. Berezin, E.T. Denisov, N.M. Emanuel, The Oxidation of Cyclohexane, Pergamon Press, Oxford, 1966.

[21] B. Hunger, M. Heuchel, L.A. Clark, R.Q. Snurr, J. Phys. Chem. B 106 (2002) 3882–3889.
[22] M. Primet, P. Pichat, M.V. Mathieu, J. Phys. Chem. 75 (1971) 1216–1221.
[23] C. Arrouvel, M. Digne, M. Breysse, H. Toulhoat, P. Raybaud, J. Catal. 222 (2004) 152–166.
[24] K. Chhor, J.F. Bocquet, C. Colbeau-Justin, Mater. Chem. Phys. 86 (2004) 123–131.
[25] H.P. Boehm, Discuss. Faraday Soc. 52 (1971) 264–275.
[26] A.P. Rivera, K. Tanaka, T. Hisanaga, Appl. Catal. B: Environ. 3 (1993) 37–44.
[27] H. Sun, F. Blatter, H. Frei, J. Am. Chem. Soc. 118 (1996) 6873–6879.
[28] H. Sun, F. Blatter, H. Frei, Catal. Lett. 44 (1997) 247–253.
[29] C.H. Hansen, G. Mul, R.B.J. Tabor, J. Royal Netherlands Chem. Soc. 112 (1993) 497–502.
[30] G. Mul, A. Zwijnenburg, B. van der Linden, M. Makkee, J.A. Moulijn, J. Catal. 201 (2001) 128–137.